Turbulence Model Sensitivity for Parachute-Like Bodies: A RANS Comparison

Puthalapattu Sukanya
puthalapattusukanya@gmail.com

***Abstract*—This paper investigates the sensitivity of computational solutions for flow over hemispherical shell geometries using different Reynolds-Averaged Navier-Stokes (RANS) turbulence models. The study aims to compare the performance of the Spalart-Allmaras (SA) and Shear-Stress Transport (SST) turbulence models on a simplified parachute test case, motivated by challenges in the stability of parachute systems in aerospace applications, such as the Orion Multi-Purpose Crew Vehicle. Using the OVERFLOW CFD solver, a hemispherical shell grid was developed to reduce computational complexity and analyze the model's impact on flow characteristics. Both models demonstrated nearly identical convergence histories and flow profiles, with minor differences attributed to grid coarseness and floating-point errors. Results indicate that the overall computational outcomes are largely independent of the chosen turbulence model for the specific grid and case. Future work will involve grid refinement and 6-DoF simulations to further explore the turbulence model's effects on dynamic forces.**

I. Introduction

This study presents a comparative analysis of computational fluid dynamics (CFD) simulations focused on flow behavior over a hemispherical shell, with specific emphasis on evaluating the influence of different Reynolds-Averaged Navier-Stokes (RANS) turbulence models. Understanding how the selection of turbulence models impacts CFD predictions is critical for improving the reliability of aerodynamic simulations, particularly for applications involving complex, unsteady flow phenomena.

A. Motivation and Background

The Orion Multi-Purpose Crew Vehicle (MPCV), developed for crewed space exploration missions, relies on a three-parachute system for controlled deceleration during atmospheric reentry in the subsonic regime. While the nominal operation of this system provides stable deceleration, real-world flight tests have revealed potential risks under off-nominal conditions, particularly when one parachute fails to deploy. In such two-parachute deployment scenarios, the spacecraft and parachute assembly may experience undesirable dynamic instabilities, including significant oscillatory motion resembling a pendulum swing. Such motion introduces critical challenges to both vehicle safety and crew survivability.[1]

To better understand and mitigate these dynamic instabilities, a combination of experimental and computational approaches has been adopted over the years. Experimental efforts include scaled drop tests, wind tunnel investigations, and full-scale structural assessments. Complementing these tests, CFD simulations have been extensively utilized to explore aerodynamic behavior under various operational conditions. For instance, static CFD analyses using the OVERFLOW solver have been performed to examine flow characteristics around rigid, non-deforming parachute geometries. These simulations typically considered single-parachute configurations in a steady-state environment, aiming to quantify parameters such as drag and static stability without accounting for large-scale body motion like pitching or swinging.[3]

While these static analyses provide valuable baseline data, they are inherently limited in capturing the complex, time-dependent forces that arise during actual dynamic scenarios. Notably, the pendulum-like motion observed under two-parachute failure conditions is driven by unsteady aerodynamic loads that vary as a function of the system's relative motion. To address this gap, the present work extends beyond static assessments by incorporating dynamic simulations where the geometry undergoes prescribed motion during the CFD run, simulating pendulum-like behavior.

To validate this dynamic modeling approach, computational results were benchmarked against experimental data from recent tests conducted at the National Full-Scale Aerodynamic Complex (NFAC) 80x120 wind tunnel facility. In these experiments, a one-third scale Engineering Development Unit (EDU) parachute, representative of the Orion MPCV's flight hardware, was anchored at the risers and controlled via tethers attached to the parachute's aft vent. Following release from the tethers, the parachute exhibited free precession within the test section, during which aerodynamic loads were measured at the riser attachments. These load data provided a means to compute aerodynamic coefficients directly, enabling validation of the CFD model's dynamic response predictions.[6]

B. Objectives of the Turbulence Model Investigation

The CFD framework employed for the aforementioned dynamic simulations utilizes a widely adopted RANS turbulence modeling approach, chosen based on its demonstrated performance in previous parachute aerodynamics studies. However, despite the routine use of such models, a systematic assessment of how sensitive the CFD results are to the specific choice of turbulence model has not been conducted for this application.

The present study addresses this gap by performing a comparative evaluation of two distinct RANS turbulence models applied to a simplified version of the parachute geometry—specifically, a hemispherical shell. This simplified configuration was selected to significantly reduce computa-

tional expense, as full-scale, high-fidelity simulations of the complete parachute system are extremely resource-intensive, often requiring hundreds of processing cores over several days to complete.

By employing this reduced-complexity model, the study aims to investigate whether variations in turbulence model selection lead to significant differences in key aerodynamic predictions, including force coefficients and flow structure characteristics. The broader goal is to assess the degree of model independence inherent to the CFD approach and to build confidence that conclusions drawn from such simulations remain valid across different RANS model formulations. Ultimately, insights gained from this study will guide the selection of turbulence models for future high-fidelity simulations involving complex, dynamic parachute systems.

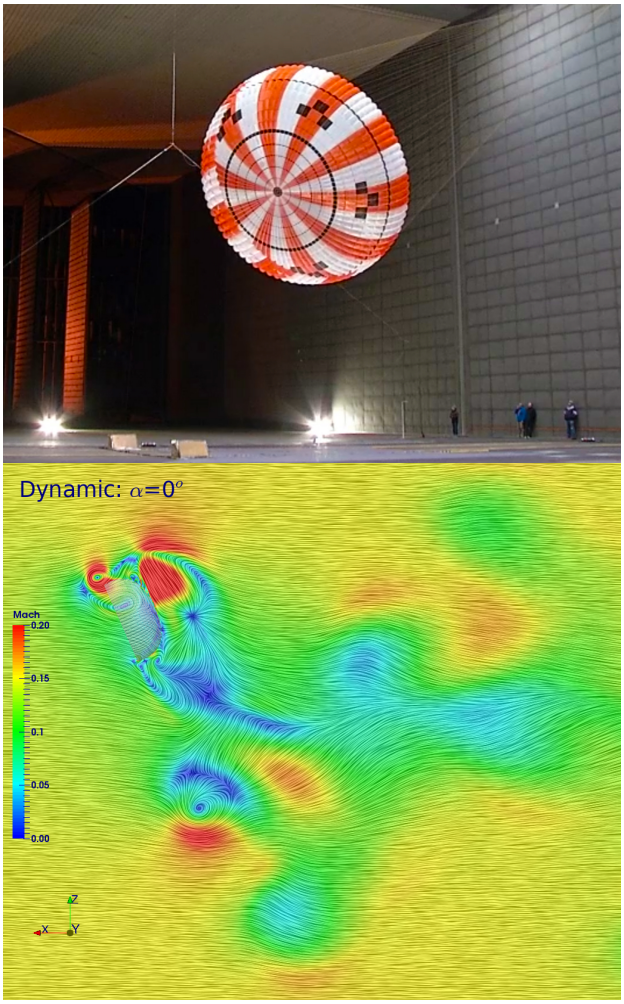

Fig. 1: Left: 1/3-scale wind tunnel test of Orion parachute. Right: CFD solution of flow over a rigid parachute exhibiting pendulum motion

II. Turbulence Study Design

A. Solver Background

CFD simulations were performed using OVERFLOW, an implicit Navier-Stokes solver, which employs finite-differencing methods on structured, overset grids.[4] Many solution algorithms and schemes are available, including Lower Upper-Symmetric Gauss Sidel (LU-SGS) implicit solution algorithm and implicit unfactored Successive Symmetric Over Relaxation SSOR algorithm. Solution scheme and algorithm is chosen to appropriately compliment the chosen turbulence model and desired solution accuracy order. OVERFLOW provides various turbulence models for use ranging from basic algebraic models to RANS methods to Large Eddy Simulation (LES). Those used in this study will be detailed in the next section.

Dual-time stepping is also employed to aid in solution convergence.[7] This process allows the solver to iterate on a steady solution between each physical time step. This aids in pre-conditioning the unsteady solution for low Mach number cases.

OVERFLOW allows for the solution of multiple species gas continuity equations to aid in the solution of chemically reactive or high Mach flows. For non-reactive flows, such as the one described in this paper, the fluid medium is treated as a single species, constant specific heat γ gas.

One major advantage of OVERFLOW's structure, overset grid nature, is that relative grid motion can be achieved without extreme additional cost as it only requires calculating new grid interpolation schemes. [5] The Geometry Manipulation Protocol (GMP) allows the user to input prescribed motion equations or let the grids react freely to aerodynamic forces according to basic equations of motion. It is for this capability that the author has selected this solver for this and the previous related study.

B. Turbulence Models

This turbulence study concerns two RANS modeling methods: the Spalart-Almaras (SA) and Shear-Stress Transport (SST) models. The SA model is a one-equation turbulence model that solves a single transport equation for a viscosity-related variable (e.g. Turbulent Kinetic Energy (TKE)).[8] In OVERFLOW, it is solved using a second-order accurate Backward Differentiation Formula (BDF2) algorithm.

The SST model is a two-equation turbulence model that expands on the SA model by solving both a convection equation accounting for the energy of the turbulence and a dissipation equation accounting for the scale of the turbulence. [2] The SST model combines the features of other two-equation models, using the $k-\omega$ method for inner boundary layer solutions and the $k-\varepsilon$ for freestream regions.

C. Case Parameters And Solution Process

The CFD case discussed in this paper was solved at the same conditions as the high-fidelity parachute simulation, which has the geometry scale as the flight parachute but a velocity scaled up by a factor of five to aid in convergence at low

Mach number. The flight Reynolds number Re is preserved by scaling down the density of the fluid medium. Flow simulations are three-dimensional as this grid will ultimately be used for six degree-of-freedom moving-mesh simulations.

Parameter	Simulation Value	Notes
Mach Number	$M = 0.15$ $(V = 1988in/s)$	Scaled up from flight
Density	$\rho = 2.61x10^{-7}slug/in^3$	Scaled down to preserve Re
Temperature	$T = 508^oR$	Yields: $\mu = 3.07x10^{-8}slug/in \cdot s$
Reynolds Number	$Re/in = \frac{\rho V}{\mu} = 16965/in$	Full: $Re = 2.36e7$
Reference Length	$L_{ref} = 1392in$	Parachute Diameter
Turbulence Models	SST, SA	NQT=205, 102

TABLE I: CFD simulation run parameters

Simulations were converged according to a three-stage process. Seeking a faster convergence than previous parachute simulations, all solution stages were time-accurate with Newton dual-time stepping from the beginning (as opposed to first converging as steady-state solution). The nondimensional physical time step size $DTPHYS$ and number of Newton subiterations $NITNWT$ for each solver stage were as follows:

Stage	DTPHYS	NITNWT
INPUT,1	0.25	5
INPUT,2	10	15
INPUT,3	2	5

TABLE II: CFD simulation convergence parameters

The first input stage was preceded by a full multi-grid process where an initial solution was converged on an extra-coarse grid.

D. Grid Design

The computational mesh was designed to maintain the primary features of the original, high-fidelity parachute model in a much simpler representation so that diagnostic simulations such as those described in this paper can be performed quickly and numerously. The same reference length was preserved from the original grid, but the parachute vent and gaps were eliminated due to their meshing complexity. The mesh was also coarsened significantly to improve convergence time, resulting in 3062742 total grid points.

The overset grid structure of the original parachute simulation was emulated as well, with multiple, cascading box grids to propagate the flow around the parachute, and one dense box grid immediately surrounding the parachute to compensate for the near-body volume grids that were inadequately small due to the concave nature of the hemisphere's shape.

III. Results

In order to compare the differences of the two turbulence models, multiple analyses techniques were employed. First, the

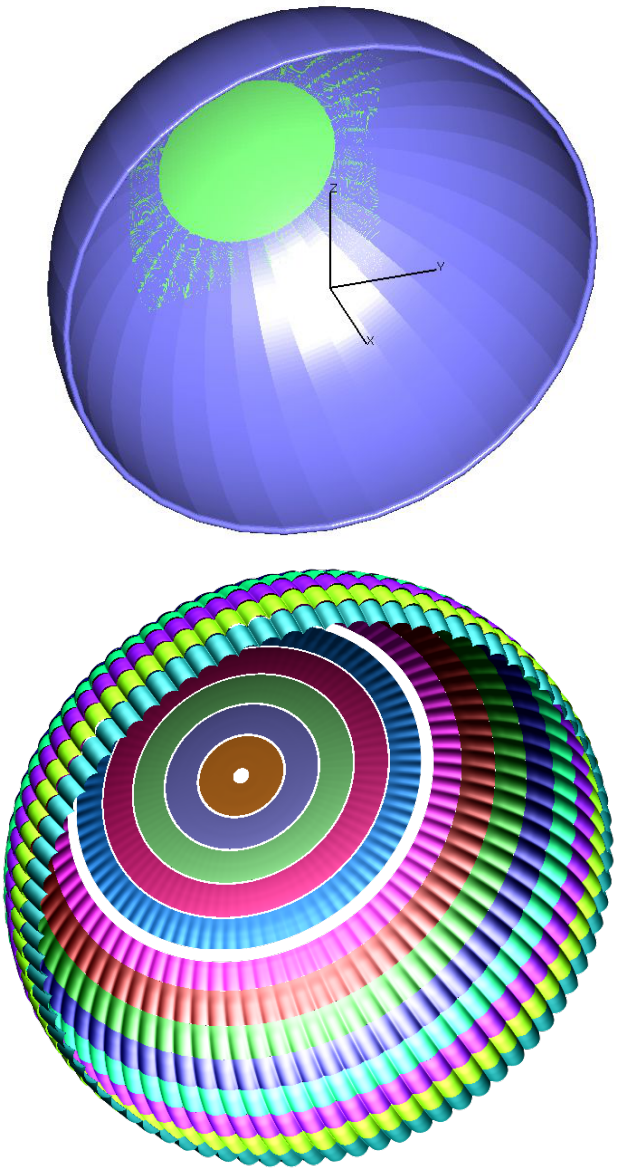

Fig. 2: Left: Simple hemispherical shell grid ($3e6$ points). Right: High-fidelity Orion MPCV parachute grid ($2e9$ points)

convergence history of various force and moment coefficients was observed, as per Fig 4.

The figure makes it obvious that there is practically no difference in the convergence histories of the two simulations. Interestingly, the change from Inputs deck 2 to 3 (at iteration 2000) shows no obvious change, despite a quartering of the physical time step. This suggests that the solution of this problem is somewhat independent of the chosen turbulence model but also indicate that there may be other factors of dependence, such as grid spacing.

Investigating the flow visually reveals some of these grid dependencies. The left image in Fig 5 demonstrates obviously contrasting regions within the grid. This is due to overlapping grid of different coarsenesses, as shown in the right image.

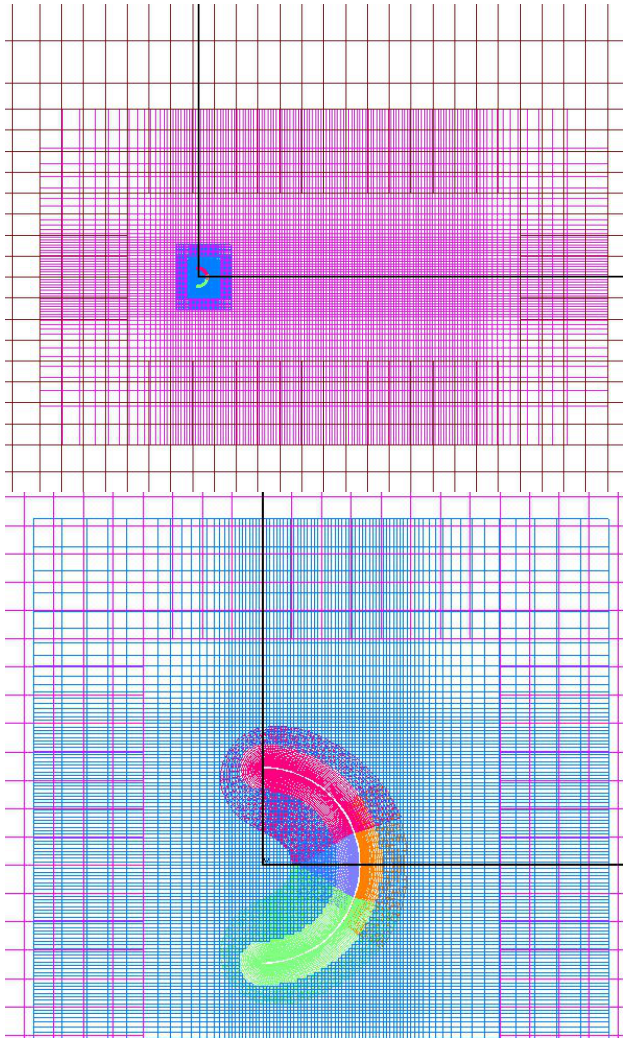

Fig. 3: Left: Off-body box grid for freestream flow around hemispherical shell. Right: Hemispherical shell body grid

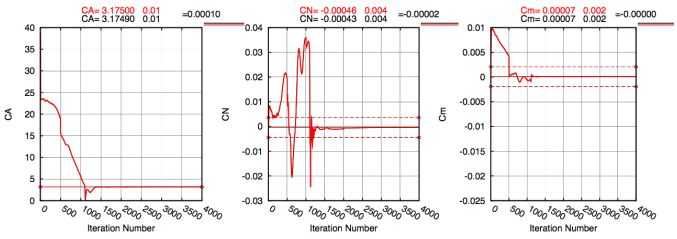

Fig. 4: Convergence history of both turbulence models showing perfect overlap (From left to right, coefficients of: axial force, normal force, and pitching moment)

Due to the highly coarse nature of this experimental grid, interpolation between grids is unideal in some locations, causing grid-dependency within the solution. Most obviously, the flow very near the hemisphere is "captured" in the very fine near-body volume grid. Eddies are well defined in this region, but are discontinuous and less resolved when crossing into other grids.

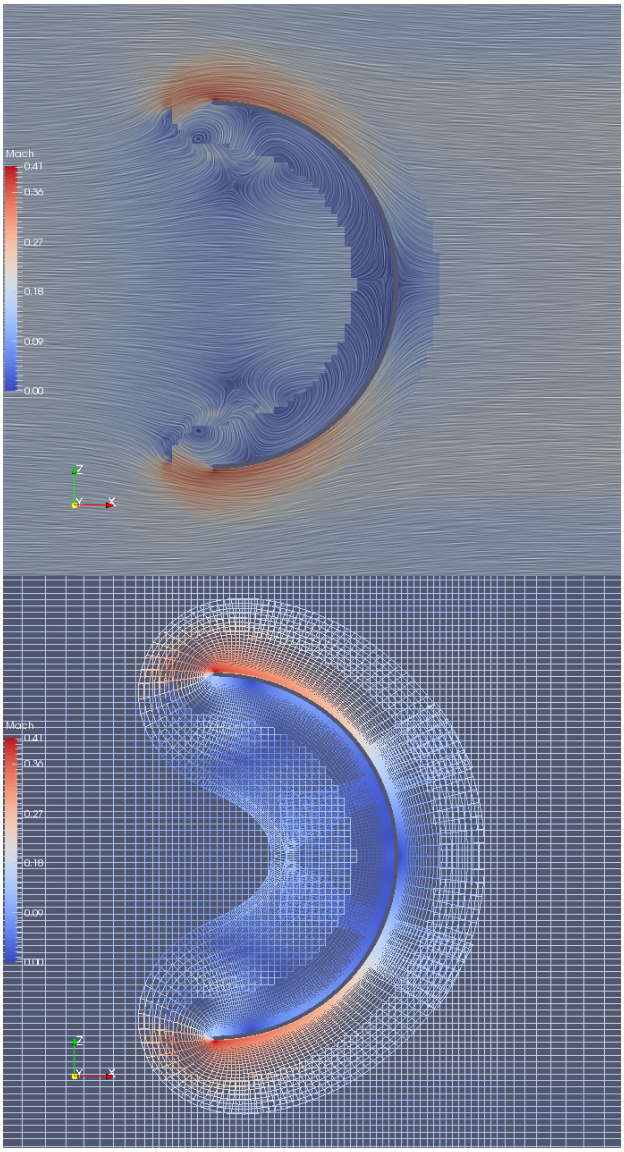

Fig. 5: Flow Mach number visualization of SST turbulence model results (SA flow essentially identical) Left: Mach contours and streamlines. Right: Mach values at grid points

Though these plots demonstrate that this grid and solution are not extremely well-conditions for production CFD, they may still serve a purpose as a turbulence model testbed. This flow was further analyzed by observing the wake x-velocity profiles created by this hemispherical body, sampled from the lines indicated below in Fig 6.

Aside from the sample locations, the above figure also reveals another flow feature indicating grid dependence: the linear flow distortion directly in front of the hemisphere caused by grid interpolation.

The plot at the end of the document in Fig **??** shows that at every streamwise station, both turbulence models have identical results. Further analysis of the difference of these

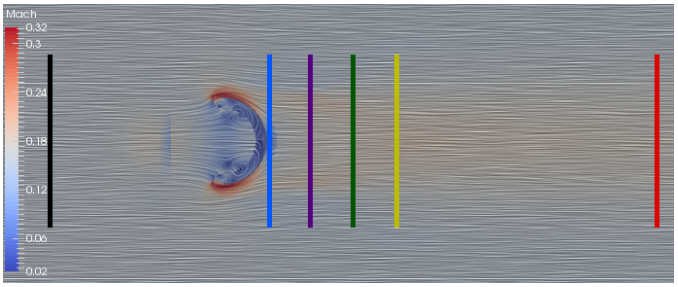

Fig. 6: Wake velocity profile sampling lines

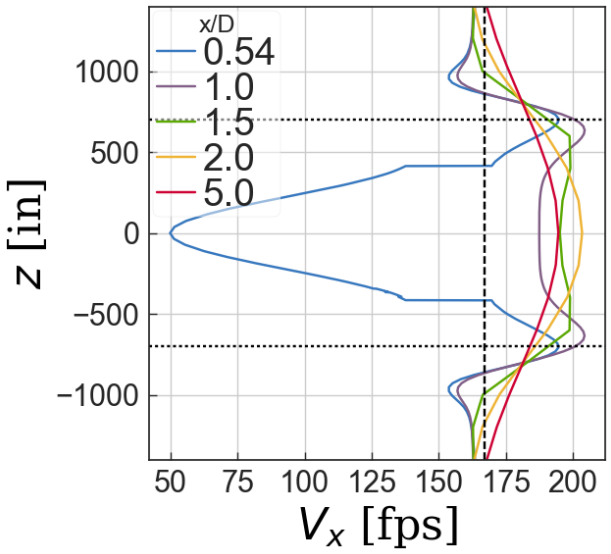

Fig. 7: Wake velocity profiles sampled at various streamwise locations for the SST simulation (Vertical dashed line is freestream velocity profile, horizontal dotted lines are edges of hemisphere geometry)

two solutions demonstrated that the only difference was due to floating point error and grid discontinuities. The image on the right shows wake velocity results for only one case. These exhibit the expected behavior of flow behind a bluff body, ranging from the most distorted just behind the hemisphere geometry and approaching the freestream distribution further downstream.

Finally, the integral effect of velocity distribution can be measured by integrating the momentum deficit to obtain a drag coefficient. For this computational simulation, the drag coefficient was computed to be $C_D = 3.2$, which is significantly higher than experimental values for a semicircle $C_D = 2.3$. Some reasonable causes for this discrepancy could be the difference between 2D and 3D flow and the general inaccuracy of RANS in modeling massively separated flow, but this result combined with the other previous observations suggests strongly that grid refinement will yield a different solution.

IV. Conclusions and Future Work

The present investigation offers valuable preliminary insights into the influence of turbulence model selection on the computational fluid dynamics (CFD) predictions for flow over a simplified, parachute-representative hemispherical shell geometry. The comparative results suggest that, under the conditions tested, the simulated aerodynamic behavior exhibits a degree of robustness with respect to the choice of Reynolds-Averaged Navier-Stokes (RANS) turbulence model. Specifically, key aerodynamic coefficients and flow characteristics remained largely consistent across the different turbulence models applied in this study.

While these findings provide encouraging evidence of model independence, it is important to emphasize that they are based on simulations performed using a relatively coarse computational grid. The use of simplified geometry and mesh resolution was intentional to reduce computational demands and facilitate this initial comparison; however, such limitations inherently restrict the ability to capture finer-scale turbulent structures and near-wall effects that may emerge under higher-fidelity conditions. It is therefore premature to draw definitive conclusions regarding the general insensitivity of parachute-relevant CFD simulations to turbulence model selection without further investigation.

Future work will focus on several key areas to build upon these initial results. First, the computational grid will undergo systematic refinement to improve spatial resolution, particularly in regions of high velocity gradients and expected flow separation. A more refined grid may reveal turbulence-dependent behaviors not captured in the current simulations, thus offering a more comprehensive understanding of model sensitivity.

In addition, the simplified hemispherical shell model utilized in this study will serve as the foundation for future dynamic simulations incorporating six degrees of freedom (6-DoF) motion. These simulations will allow the geometry to undergo realistic pendulum-like oscillations, closely resembling the dynamic instabilities observed during parachute deployments with incomplete inflation scenarios. By integrating dynamic motion into the CFD framework, it will be possible to evaluate how turbulence model selection influences unsteady aerodynamic loads and system stability under more complex, time-dependent conditions.

Furthermore, validation of the refined CFD simulations will be pursued through continued comparison with experimental data from wind tunnel testing, such as those performed at the National Full-Scale Aerodynamic Complex (NFAC). Such comparisons are essential to ensure the credibility of the computational predictions and to guide improvements in both modeling approaches and physical understanding of parachute aerodynamics.

Ultimately, the insights gained from this research will contribute to the development of more reliable and predictive CFD methodologies for parachute systems. This, in turn, has the potential to enhance the safety and performance of critical

aerospace applications, such as crewed reentry vehicles, where dynamic stability is of paramount importance.

REFERENCES

[1] E. S. Ray and R. A. Machin, "Pendulum Motion in Main Parachute Clusters," in *23rd AIAA Aerodynamic Decelerator Systems Technology Conference*, Submitted, 2015.

[2] F. R. Menter and Christopher L. Rumsey, "Assessment of Two-Equation Turbulence Models for Transonic Flows," in *25th AIAA Fluid Dynamics Conference*, Submitted, 1994.

[3] J. S. Greathouse and A. M. Schwing, "Study of Geometric Porosity on Static Stability and Drag using Computational Fluid Dynamics for Rigid Parachute Shapes," in *23rd AIAA Aerodynamic Decelerator Systems Technology Conference*, Submitted, 2015.

[4] R. H. Nichols, R. W. Tramel, and P. G. Buning, "Solver and Turbulence Model Upgrades to OVERFLOW 2 for Unsteady and High-Speed Applications," No. AIAA 2006-2824, 2006.

[5] S. M. Murman, W. M. Chan, M. J. Aftosmis, and R. L. Meakin, "An Interface for Specifying Rigid-Body Motions for CFD Applications," AIAA Paper 2003-1237, 2003.

[6] J. M. Macha and R. J. Buffington, "Wall-Interference Corrections for Parachutes in a Closed Wind Tunnel," *Journal of Aircraft*, Vol. 27, No. 4, pp. 320-325, April 1990.

[7] Pandya, S. A., Venkateswaran, S., and Pulliam, T. H., "Implementation of Preconditioned Dual-Time Procedures in OVERFLOW", AIAA-2003-0072, Jan. 2003.

[8] P. R. Spalart and S. R. Allmaras., "A One-Equation Turbulence Model for Aerodynamic Flows", AIAA-92-0439, January 1992.